Monte Carlo Calculation of Phase Equilibria for a Bead-Spring Polymeric Model

Yu-Jane Sheng and Athanassios Z. Panagiotopoulos*

School of Chemical Engineering, Cornell University, Ithaca, New York 14853-5201

Sanat K. Kumar

Department of Materials Science and Engineering, Polymer Science Program, The Pennsylvania State University, University Park, Pennsylvania 16802

Igal Szleifer

Department of Chemistry, Purdue University, West Lafayette, Indiana 47907

Received August 10, 1993; Revised Manuscript Received October 25, 1993®

ABSTRACT: Vapor-liquid phase diagrams for a bead-spring polymeric model have been calculated for chain lengths of 20, 50, and 100 from Monte Carlo simulations using the recently proposed chain increment method (Kumar *et al. Phys. Rev. Lett.* **1991**, *66*, 2935) to determine the chain chemical potentials. Densities of both phases at coexistence and vapor pressures were obtained directly for a range of temperatures from highly subcritical to the vicinity of the critical point, and the critical temperature and density for each chain length were obtained by extrapolation. We also calculated the second virial coefficients for chain-chain interactions of our model and found that the temperature at which the second virial coefficient vanishes for long chains coincides, within computational uncertainty, with the infinite chain length critical point from our phase equilibrium results. At the critical points of the finite length chains the second virial coefficient assume negative values, indicating attractive interchain interactions. The radius of gyration of chains of varying length was also determined and the Θ temperature obtained from the radii of gyration found to coincide, within computational uncertainty, with the critical point for an infinite chain length polymer. The computational methodology we utilize can be extended to the calculation of phase equilibria in multicomponent polymer/solvent systems.

I. Introduction

Thermodynamics of polymeric systems are commonly modeled through the use of the mean-field Flory-Huggins theory which is currently 50 years old.[1-3] According to this theory, the critical temperature, T_c, and the critical volume fraction, φ_c, for the vapor-liquid coexistence of a pure polymer (or, consequently, of the phase separation in polymer solutions) are predicted to follow universal power law scaling relationships with chain length n,

$$T_c - \Theta \propto \varphi_c \propto n^{-0.5} \tag{1}$$

where Θ is the critical temperature for chains of infinite length. Equation 1 has not been verified to date from simulations, primarily because of the difficulty in obtaining phase coexistence properties for polymeric models.

Previous investigations of phase diagrams for chain systems by simulation include the lattice calculations of Madden *et al.*[4] In that study the equilibrium between two lattice polymer solutions, one concentrated in polymer and the other in holes, was achieved through the diffusion of molecules across the interphase between the two coexisting phases. While this method provides for a direct determination of phase coexistence it nevertheless suffers from the disadvantages that the interphase constitutes a significant part of the simulated system and that polydispersity has to be introduced to facilitate the equilibration of the simulated sample. In addition, it is difficult to obtain information on the properties of the dilute (gas) phases from interfacial simulations except in the immediate vicinity of the critical point. Despite these limitations this work is the only one to date to compare theoretical and simulation results for phase coexistence in one-component macromolecular systems. In a study less directly related to the present work Sariban and Binder[5] have studied coexistence in symmetric binary polymer blends. The Monte Carlo technique used by Sariban and Binder takes advantage of the symmetry of the system to enable determination of the phase boundary.

An alternative to direct interfacial simulations is the calculation of the free energies (and hence phase diagrams) of polymer chains from simulations. A technique commonly used for this purpose for small-molecule systems is the Widom test particle method[6] that requires insertions of a "test" polymer chain into a snapshot of the system of interest. This procedure becomes significantly less efficient as the density and chain lengths are increased.[7] Frenkel and co-workers[8,9] and de Pablo *et al.*[10] have proposed novel biased insertion procedures, based on the Rosenbluth and Rosenbluth algorithm for lattice polymers,[11] that can be used to estimate the chemical potentials of polymer chains. Because a complete chain is still inserted in these schemes, sampling difficulties are encountered for longer chains at high densities.[12] A combination of configurational biased sampling and the Gibbs ensemble[13] has enabled direct calculations of phase coexistence for chain molecules.[14] This technique has recently been used[15] for the calculation of phase diagrams for alkanes up to C_{48}, suggesting that these more convenient techniques are relevant even for chains of moderate length.

Several workers have investigated chain dimensions and partition functions for isolated chains on a lattice, as well as in free space.[16-20] Through these and previous studies it has been clearly established that there exists a special temperature where a chain of infinite length assumes "random flight" conformations. The numerical value of this temperature is sensitive to the details of the potential parameters in the model. Long chains at all lower temperatures assume collapsed conformations, while

® Abstract published in *Advance ACS Abstracts*, December 1, 1993.

0024-9297/94/2227-0400$04.50/0

chains assume self-avoiding statistics at all higher temperatures. Since collapsed conformations involve much larger number of polymer–polymer contacts, it has also been argued that the second virial coefficients for long chains, characterizing chain–chain interactions in the zero density limit, also change sign at this temperature. These arguments therefore suggest[21,22] that this special temperature should also be the critical temperature for a chain of infinite length, defined by Flory as the Θ temperature. This assertion, however, has not been verified to date from computer simulations on continuous-space models. Lattice-based calculations[38] have confirmed the equivalence of the temperature at which chain dimensions behave quasi-ideally and the temperature for the vanishing chain–chain second virial coefficient at the limit of long chains. However, there are no suitable phase equilibrium results for lattice models to include the critical point for phase separation in these comparisons.

Much interest therefore remains in obtaining the thermodynamic and phase equilibrium behavior for model polymer systems to which theories can be compared. In this paper, we focus on the simple case of the vapor–liquid equilibrium (VLE) of a continuous-space model homopolymer system, where chains are modeled as beads connected by stiff springs. In addition to its implications on the calculation of the VLE phase diagrams of pure oligomeric chains, which are of relevance for petroleum processing applications,[23] this calculation is also of import due to its direct connection to the phase equilibria of binary polymer/solvent systems.[24] The key method in the present work is the recently proposed chain increment method,[25] according to which the chemical potentials of whole chains are obtained by adding the contributions for all chains shorter than the desired length. Potential sampling difficulties associated with biased insertion procedures are thus avoided, and we can perform calculations for significantly longer chain lengths than are possible with methods that rely on insertions of whole chains. The phase diagrams obtained from this procedure are in principle exact to within statistical uncertainties. We obtain the coexisting phase densities and vapor pressures for chains of length 20, 50, and 100 for a range of temperatures and compare these results to approximate phase diagrams of Panagiotopoulos.[29] We extrapolate the results to the critical point using scaling relationships to obtain the chain length dependence of the critical temperature and density. We also address the issue of the equivalence of the infinite chain length critical temperature and the temperature at which the chain–chain second virial coefficient vanishes and chain dimensions are unperturbed. Our results indicate that all three temperatures coincide within computational uncertainty, providing additional support for the Flory conjecture.

II. Model and Simulation Methods

Model. Polymer chains were modeled as beads connected by stiff springs as in previous work.[25] Nonbonded beads interact through the standard Lennard–Jones potential,

$$U_{nb} = 4\epsilon\left[\left(\frac{\sigma}{r}\right)^{12} - \left(\frac{\sigma}{r}\right)^{6}\right] \qquad (2)$$

where ϵ and σ are the energy and size parameters, respectively. All reduced quantities that appear in the results section and are denoted by a superscript (*) are obtained by using the monomeric ϵ and σ as reducing parameters. The potential was truncated at a distance of half the simulation box length, and long-range corrections were added to all calculated thermodynamic quantities assuming that the segment–segment radial distribution function is unity for distances greater than half the box length.[26] The interactions between bonded beads were represented by a harmonic spring potential as

$$U_b = \frac{1}{2}\kappa(r-\sigma)^2 \qquad 0.5 < \frac{r}{\sigma} \le 1.5 \qquad (3)$$

The potential is infinite elsewhere. We have chosen $\kappa\sigma^2/\epsilon = 400$, consistent with previous studies.[25]

Simulation Details. The systems simulated in this work consisted of a collection of chains of length n in a cubic box. Periodic boundary conditions were assumed in all three directions, and the systems contained 800–1000 beads depending on the length of the chains employed. Due to computing time considerations it would be truly difficult to study much bigger systems. Much smaller systems cannot be meaningfully studied because of the polymeric nature of the systems under study. The properties of interest for phase equilibrium calculations (chemical potential, pressure) are expected to be less sensitive to system size than properties such as chain dimensions. The simulations were mostly performed under conditions of constant temperature, pressure, and total number of particles, but a few runs were performed at constant volume to determine low-density gas phase properties.

The initial configuration for the first temperature studied for a given chain length was a random one obtained by growing the chains to the desired length and density and was equilibrated for 10–20 million Monte Carlo steps. Runs for the same chain length at different temperatures were performed starting with the final configuration from a previous temperature and were equilibrated for 5–10 million steps. The production period for each simulation was between 5 and 8 million Monte Carlo steps.

The moves employed in our simulations were reptation and bead displacement motions. In the reptation moves an end was picked at random, removed, and placed at the other end in a random orientation at a distance r chosen in the interval $0.5\sigma < r \le 1.5\sigma$. The distance was chosen with probability proportional to r^2 so as to satisfy the condition of equal sampling of all points in the spherical shell surrounding the destination end. Bead displacement moves involve randomly picking a bead and displacing it to a new position in the vicinity of the old position. This move, which is the analog of the "crankshaft" moves used in simulations of bead–rod chains, facilitates the equilibration of the central parts of the chain molecules. The new configurations resulting from reptation or bead displacement moves were accepted according to the standard Metropolis acceptance criterion with a probability of acceptance, P_{acc}, given by

$$P_{acc} = \min\left[1, \exp\left(\frac{-\Delta U}{k_B T}\right)\right] \qquad (4)$$

where ΔU is the change in the total energy of the system due to the move, k_B is the Boltzmann constant, and T is the absolute temperature.

An important issue for all Monte Carlo studies of polymeric models is whether the moves used adequately sample configuration space. The model we are employing in this study involves significantly fewer constraints to the motion of internal beads than realistic models that include bond angle and torsional potential terms. We have verified, by visual inspection of individual chains as a function of Monte Carlo steps generated that significant loss of correlation between initial and final positions and conformations occurs, even for the lowest temperatures

and highest densities studied.

To maintain constant pressure, the volume of the simulation box was also allowed to fluctuate. Random volume changes were made according to the equation

$$V' = V + \delta V_{max}(2\xi - 1) \tag{5}$$

with ξ a uniformly distributed random number in the interval (0,1). δV_{max} governs the maximum change in volume of the simulation box and is chosen to result in an average acceptance ratio for the volume changes of 50%. Typical values of δV_{max} are around 1% of the volume of a liquid phase. V and V' are the old and new volumes, respectively. The coordinates of the molecules are changed by scaling the centers of mass for each chain to the new volume. The new state is accepted with probability

$$P_{acc} = \min\left\{1, \exp\left[-\frac{\Delta U + P(V' - V)}{k_B T} + N \ln \frac{V'}{V}\right]\right\} \tag{6}$$

where ΔU is the internal energy difference between the new and old states and N the number of chains in the system.

The pressure for our systems was calculated via the molecular definition of the virial,[26] which involves only interchain nonbonded interactions. The stiff harmonic potential between bonded beads does not therefore contribute to fluctuations of the calculated virial and the statistical accuracy improves significantly with respect to a calculation based on the atomic virial.

Chain Increment Method. The calculation of the chemical potentials for the polymer chains is based on the chain increment method proposed by Kumar et al.[25] For a chain of length x present in infinite dilution in an appropriate medium (in our calculations a homopolymer composed of chains of length n at density ρ) the incremental chemical potential,[27,28] $\mu_r^+(x)$, is given by

$$\mu_r^+(x) = -kT \ln \langle \exp(-\beta U_{x+1}^+) \rangle \tag{7}$$

where U_{x+1}^+ is the energy experienced during growth of the chain from length x to length $x + 1$. In our simulations we calculated the energies that enter in the ensemble average of eq 7 during attempted reptation moves, from the energy experienced by the added bead at the end of the chain. The total chemical potential of a chain of length n can be obtained by sequentially summing the incremental chemical potentials of all chains of shorter length,

$$\mu_r^{chain}(n) = \sum_{x=1}^{n} \mu_r^+(x) \tag{8}$$

In principle, n different simulations need to be performed in order to obtain the chain chemical potential of a chain of length n according to eq 8. In practice, the chain length dependence of the chemical potential for bead–spring models is found to be weak,[28] and a significantly reduced number of simulations is required. Figure 1 presents a typical variation of incremental chemical potential versus chain length for growing a single chain of variable length in a medium of 100 mers at a liquidlike and a gaslike density. For all other cases examined the chain length dependence of the incremental chain potential was also found to be weak above a chain length of approximately 10 segments. This is in contrast to the behavior of the incremental chemical potential for a realistic chain model[10] which was observed to approach an asymptotic value only for significantly longer chains.

A previous approximate calculation of phase diagrams for the bead–spring model we are using has been performed

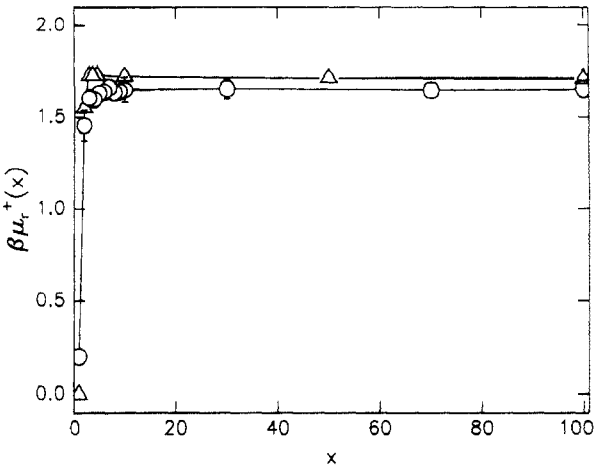

Figure 1. Incremental chemical potential, $\beta\mu_r^+(x)$, for a single growing chain in a medium of 100 mers at $T^* = 3.3$ as a function of chain length x: (△) reduced density $\varphi = 0.0002$; (○) $\varphi = 0.412$. Lines are drawn through the points for visual clarity. Error bars are shown only when greater than the symbols.

by Panagiotopoulos and Szleifer.[29,30] In that calculation, the chain length dependence of the chemical potential was ignored and the sum in eq 8 approximated by $n \times \mu_r^+(n)$. Although we expected this approximation to be an asymptotically better estimate for the chemical potentials of longer chain length polymers, its consequences on the calculated phase diagrams of the relatively short chain length polymers considered ($n \leq 100$) was unclear.

Determination of Phase Coexistence. For a specified temperature in a one-component system the conditions of thermodynamic equilibrium between two phases require equality of pressure and chemical potential. We determine the coexisting vapor and liquid densities by a calculation procedure similar to that described by Fisher *et al.*[31] that involves the following steps.

Step 1. Perform a series of incremental chemical potential calculations for chains of increasing length in a solvent of n mers for the liquid at constant pressure, $P^* = 0$, and obtain the residual chemical potential of the chains in the liquid, $\mu_{r,liq}^{chain}$.

Step 2. Perform a constant-volume calculation for the gas at a low density for which interchain interactions are negligible and obtain $\mu_{r,gas}^{chain}$.

Step 3. Estimate the molar density of the gas coexisting with the liquid, ρ_{gas}, by matching the total chemical potentials of the liquid and gas phases

$$\mu_{r,gas}^{chain} + k_B T \ln \rho_{gas} = \mu_{r,liq}^{chain} + k_B T \ln \rho_{liq}$$

Step 4. If needed, calculate corrected values for the coexistence pressure and chemical potential of the gas at the density ρ_{gas} calculated in step 3 by performing a constant-volume simulation in the gas phase.

Step 5. Go to step 1 using the new estimated coexistence pressure and density of the gas phase.

This iterative procedure is continued until the pressure and chemical potential of both phases are equal to within their respective statistical uncertainties. For most temperatures we have studied, the gas phase is of sufficiently low density that this procedure converges without iteration. For temperatures close to the critical point the required number of iterations increases to 2 or 3.

Calculation of Chain–Chain Second Virial Coefficients. To determine the relationship between the phase behavior of a polymeric system composed of many chains and the behavior of isolated chains, we performed a calculation of the chain–chain second virial coefficient as

a function of chain length and temperature. At the limit of long chain lengths, it is commonly believed that the temperature at which the second virial coefficient becomes zero coincides with the critical temperature.[1] We determine the chain–chain second virial coefficients from low temperature volumetric data using the relationship

$$A_2 = \lim_{\rho \to 0} \left[\frac{\partial Z}{\partial \rho} \right]_T \tag{9}$$

where Z is the compressibility factor ($Z = P/\rho kT$).

At low densities reptation and internal bead displacement moves are not very efficient in achieving large-scale motion of the chains and adequate sampling of configuration space required for an accurate determination of chain–chain second virial coefficients. In order to obtain good statistics at low densities, we supplement reptation and crankshaft moves with whole chain displacements that move the center-of-mass of a chain without changing its internal configuration.

Determination of Unperturbed Chain Dimension Temperatures. A final quantity of interest for our systems is the behavior of the radius of gyration as a function of temperature in the vicinity of the critical point. It is widely believed that at the Θ temperature, that is the critical temperature at the limit of infinite chain length, sufficiently long chains behave quasi-ideally, that is $\langle R_g^2 \rangle \propto n$. Determining the behavior of the radius of gyration as a function of chain length and temperature provides insight into the relationship between conformational properties and phase equilibria in our systems.

The root-mean-squared radius of gyration of isolated polymer chains was determined for our model for chain lengths up to 1000 segments. To sample phase space efficiently, the polymer chains were moved through "pivot" moves as well as reptation and crankshaft displacement moves. During pivot moves a bead is selected at random, thus defining two sections of the polymer of generally unequal length. One of the two sections is selected at random and an attempt is made to rotate the selected section in a random direction. Approximately 5 million Monte Carlo steps were generated at every temperature for each chain length. The mean radius of gyration was calculated by

$$\langle R_g^2 \rangle = \frac{1}{M} \sum_{j=1}^{M} \left(\frac{1}{n} \sum_{i=1}^{n} (\vec{r}_{j,i} - \vec{r}_{j,\mathrm{cm}})^2 \right) \tag{10}$$

where $\vec{r}_{j,i}$ is the position of segment i in configuration j, $\vec{r}_{j,\mathrm{cm}}$ is the center-of-mass position, and M is the total number of configurations generated with Metropolis sampling.

III. Results and Discussion

Figure 2 gives the calculated vapor–liquid phase diagrams of the bead–spring chain model for chain lengths $n = 20$, 50, and 100 mers, respectively, from bottom to top. As the chain length increases, the phase envelopes become skewed toward the $\rho^* = 0$ axis and the critical temperature increases. These observations are in qualitative agreement with experimental data for polymer/solvent systems.[32,33] Table 1 gives the properties of the coexisting phases, including information on the coexisting volume fractions, $\varphi = n\rho^*$, where n is the chain length and ρ^* the reduced molar density, reduced vapor pressures, chemical potentials, and internal energies of the liquid and gas phases. Because of the indirect technique by which the coexisting phase properties were estimated, it is difficult to obtain an accurate measure of the uncertainty in the calculated gas phase density. We estimate that the gas phase densities reported are accurate to approximately 20% of the reported value.

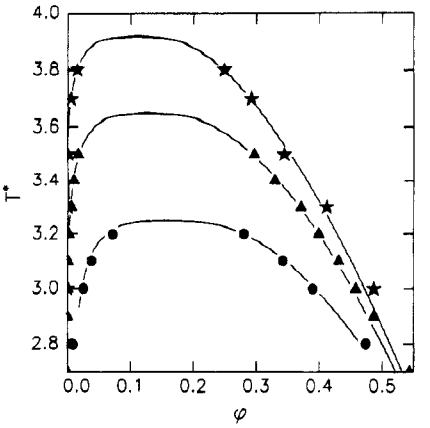

Figure 2. Reduced temperature versus reduced density at coexistence. Monte Carlo results: (★) $n = 100$; (▲) $n = 50$; (●) $n = 20$. Fitting of Monte Carlo results to scaling relationships (eq 11) with $\beta = 0.332$: (—).

Table 1. Results for Phase Coexistence Envelope of Chains of Length n = 20, 50, and 100[a]

T^*	φ_{liq}	φ_{gas}	P^*_{sat}	U^*_{liq}	U^*_{gas}	$\beta\mu^+_{\mathrm{r,liq}}$	$\beta\mu^+_{\mathrm{r,gas}}$
			$n = 20$				
2.5	0.557(9)	0.0010	$1.2(5) \times 10^{-4}$	−1.69(7)	0.49(3)	1.47(2)	1.758(6)
2.8	0.474(7)	0.0075	$9.4(6) \times 10^{-4}$	−1.03(4)	0.71(3)	1.55(3)	1.748(5)
3.0	0.390(8)	0.025	$2.7(9) \times 10^{-3}$	−0.61(2)	0.70(2)	1.58(4)	1.712(7)
3.1	0.342(9)	0.038	$5(1) \times 10^{-3}$	−0.35(5)	0.68(2)	1.59(4)	1.701(7)
3.2	0.281(9)	0.062	$8(4) \times 10^{-3}$	−0.05(1)	0.65(3)	1.61(4)	1.682(8)
			$n = 50$				
2.7	0.543(6)	0.00003	$1.7(7) \times 10^{-6}$	−1.42(1)	0.43(2)	1.57(3)	1.740(4)
2.9	0.487(7)	0.0001	$5.9(9) \times 10^{-6}$	−1.01(2)	0.57(2)	1.59(3)	1.732(5)
3.1	0.431(7)	0.001	$6(2) \times 10^{-5}$	−0.65(3)	0.74(1)	1.61(4)	1.720(5)
3.2	0.400(8)	0.002	$1(2) \times 10^{-4}$	−0.42(3)	0.82(2)	1.62(4)	1.710(4)
3.3	0.371(7)	0.0055	$3(2) \times 10^{-4}$	−0.27(2)	0.84(1)	1.63(4)	1.708(5)
3.4	0.329(9)	0.0096	$5(3) \times 10^{-4}$	−0.01(2)	0.93(3)	1.63(3)	1.696(5)
3.5	0.30(1)	0.017	$9(6) \times 10^{-4}$	0.18(3)	0.96(3)	1.64(4)	1.689(6)
			$n = 100$				
3.0	0.486(7)	0.00001	$3(2) \times 10^{-7}$	−0.93(3)	0.51(3)	1.62(3)	1.721(8)
3.3	0.412(8)	0.00023	$7(6) \times 10^{-6}$	−0.38(2)	0.79(1)	1.65(2)	1.706(9)
3.5	0.344(8)	0.0011	$2(2) \times 10^{-5}$	0.04(3)	0.98(3)	1.65(3)	1.695(8)
3.7	0.292(9)	0.0052	$1(2) \times 10^{-4}$	0.29(3)	1.07(2)	1.65(4)	1.682(7)
3.8	0.25(1)	0.015	$4(3) \times 10^{-4}$	0.58(4)	1.10(3)	1.65(4)	1.656(7)

[a] The columns give the reduced temperature $T^* = k_B T/\epsilon$, volume fractions $\varphi = n\rho\sigma^3$ (where ρ is the molar density), reduced saturated vapor pressures, $P^*_{\mathrm{sat}} = P_{\mathrm{sat}}\sigma^3/\epsilon$, reduced internal energies, $U^* = U/\epsilon$, and the limiting values of the incremental chemical potential, $\beta\mu^+_r$ for the coexisting liquid and gas phases. The numbers in parentheses indicate the estimated error in the last decimal digit: 0.58(4) means 0.58 ± 0.04.

Critical points were estimated by fitting the results for liquid and vapor densities to the rectilinear diameter rule and the scaling relationship for the width of the coexistence curve,

$$\frac{\rho_{\mathrm{liq}} + \rho_{\mathrm{gas}}}{2} = \rho_c + A(T_c - T)^{\mu} \tag{11}$$

$$\rho_{\mathrm{liq}} - \rho_{\mathrm{gas}} \propto (T_c - T)^{\beta}$$

Dobashi *et al.*[32] have determined values of β from experimental data on the polystyrene/methylcyclohexane binary system. For the lower molecular weight solutions studied by Dobashi *et al.* scaling of the form of eq 11 with a value of β appropriate for the Ising universality class in three dimensions was observed over a relatively wide temperature range. Previous simulation studies of vapor–liquid equilibria of small-molecule systems[34] have also established that the shape of the computed coexistence

Table 2. Estimated Critical Temperatures, Critical Volume Fractions, and Reduced Critical Pressure for Chains of Length n = 20, 50, and 100 Using the Scaling Relationships (eq 11) with β = 0.332 and μ = 1[a]

n	T_c^*	φ_c	P_c^*
1	1.32	0.304	0.134
20	3.25	0.164	0.01
50	3.65	0.134	0.003
100	3.92	0.115	0.0007
∞	4.59	0.0	0.0

[a] The infinite-chain length critical temperature is obtained by extrapolation using the Schultz-Flory relationship.[35] Critical properties of pure Lennard-Jones monomers are taken from ref 13.

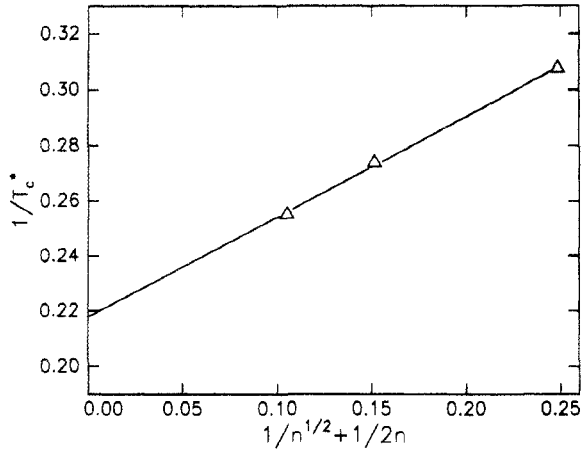

Figure 3. Inverse reduced critical temperature versus the quantity $(1/\sqrt{n}) + (1/2n)$. The straight line is a linear least-squares fit through the data.

curve close to the critical point follows eq 11 with the universal value of β up to distances significantly removed from the critical point. Our data are not sufficiently near the critical point to be useful in determining the value of β independently—any value in the range $\beta = {}^1/_2$–$^1/_3$ will give fits of the coexistence curves of approximately comparable quality. However, because of the evidence mentioned above, we chose to obtain estimates of the critical points by using the values of the exponent β = 0.332 recommended by Dobashi *et al.* Consistent with previous practice,[34] we chose μ = 1.

The estimated location of the critical points from the scaling relationships for the three chain lengths studied are listed in Table 2. The critical properties for a pure Lennard-Jones fluid are also included for comparison.[13] It is of significant interest to extrapolate the results to longer chain lengths and obtain an estimate of the infinite molecular weight critical temperature for our model. Experimental results for the dependence of critical temperature on chain length are often plotted as $1/T$ versus $(1/\sqrt{n}) + (1/2n)$, in a Schultz-Flory diagram.[35] According to Flory theory, such a diagram should result in a straight line. Although we have only three points, making it difficult to draw definite conclusions, our results presented in Table 2 and Figure 3 lie on an approximately straight line when plotted in this fashion. By extrapolation to zero abscissa in the Schultz-Flory diagram, we estimate the critical temperature for infinite chain length for our model as $T_c^\infty = 4.59$.

The apparent dependence of the critical volume fraction on chain length from our results is $\varphi_c \propto n^{-0.22}$. Flory-Huggins theory predicts that $\varphi_c \propto n^{-1/2}$. Experimental data by Dobashi et al.[32] and Shinozaki et al.[33] show a molecular weight dependence of the critical volume fraction weaker than that of the Flory-Huggins theory as

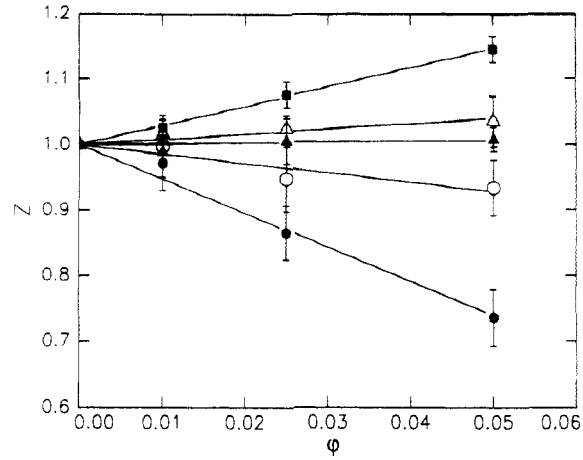

Figure 4. Compressibility factor, Z, vs reduced density, φ, for chains of length n = 20: (●) T^* = 3.25; (○) T^* = 4; (▲) T^* = 4.3; (△) T^* = 5; (■) T^* = 6.

$\varphi_c \propto n^{-0.38}$ and $n^{-0.4}$, respectively. If only the shorter chain lengths in the experimental results are used in regressing a value for the exponent governing the critical volume fraction versus chain length dependence, we also obtain an effective exponent value lower than the value obtained from higher chain lengths. We therefore argue that our data for the critical density are not in the scaling regime, and the calculated value of the exponent is an underestimate of its value for longer chain lengths. This, however, does not appear to be the case for the critical temperature data.

It is of interest to compare the results obtained from the present results with the approximate calculations of Panagiotopoulos,[29] obtained by ignoring the chain length dependence of the chemical potential. The approximate calculations require 1–2 orders of magnitude less computational effort and can be used to obtain the main features of the phase diagrams and a reasonable location of the critical point. The density of the liquid phase at coexistence is determined primarily by the condition of essentially zero pressure (except very close to the critical point), and there is good agreement between the present results and the previous approximate calculations for this quantity. For the gas phase densities there are discrepancies between approximate and present calculations that increase with chain length. For n = 100, the difference between the two sets of results is approximately a factor of 10, reflecting the different chemical potential dependences on chain length in the gas and liquid phases.

According to Flory-Huggins theory,[1] the infinite molecular weight critical temperature, T_c^∞, is also the point where the polymer-polymer second virial coefficient vanishes. To verify the critical properties we have obtained from extrapolating the vapor-liquid equilibrium phase behavior, we have also conducted simulations to obtain the Boyle temperatures for different chain lengths. We obtain the second virial coefficient from pressure vs volume data at low densities. Figure 4 shows typical results obtained for the compressibility factor versus densities for chains of length n = 20. The slopes of these lines give the chain–chain second virial coefficient, A_2. The densities used in the determination of the second virial coefficient were significantly below the overlap concentration, c^*, calculated according to deGennes[36] as $c^* \sim n^{-0.8}$. This scaling relationship is valid for chains in the good solvent regime and therefore provides a lower limit to the overlap concentration of our systems. Bruns[38] and Janssens *et al.*[37] observed that the Boyle temperature of chains on a 5-choice cubic lattice is a weak function of chain length.

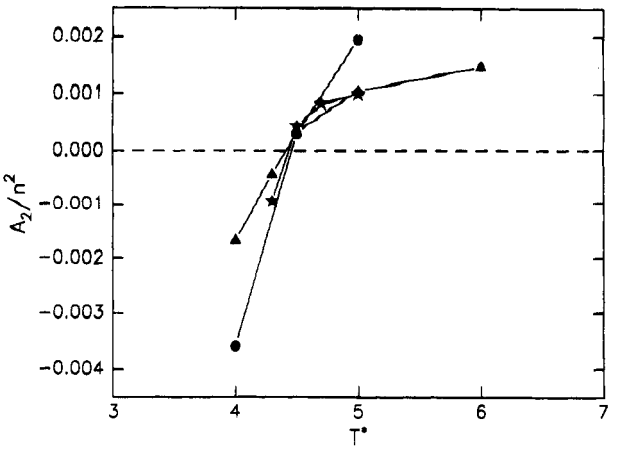

Figure 5. Chain–chain second virial coefficients, A_2, versus reduced temperature, T^*, for various chain lengths: (★) $n = 100$; (▲) $n = 50$; (●) $n = 20$.

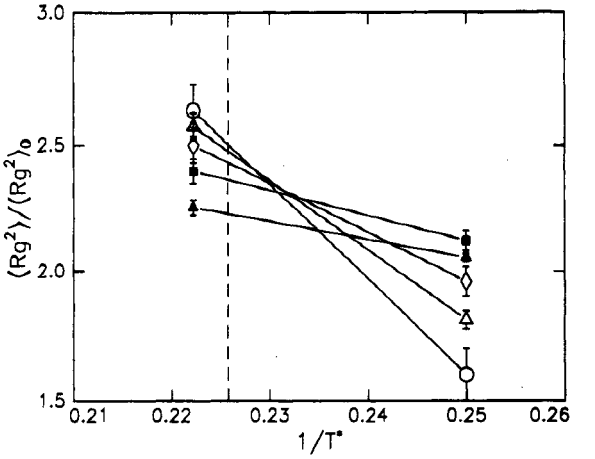

Figure 6. Reduced mean radius of gyration $\langle R_g^2\rangle/\langle R_g^2\rangle_0$, where $\langle R_g^2\rangle_0 = n(n+2)\sigma^2/6(n+1)$ as a function of inverse reduced temperature, $1/T^*$: (■) $n = 100$; (▲) $n = 200$; (◇) $n = 300$; (△) $n = 500$; (○) $n = 1000$.

As shown in Figure 5, the Boyle temperatures at which $A_2 = 0$ for our continuous-space model are chain length dependent, but the dependence is fairly weak. The estimated temperature for the Boyle temperature at the limit of long chain lengths is 4.43 ± 0.1. This result is within 4% of $T_c^\infty = 4.59$, calculated from the phase equilibrium data.

An important observation is that at the critical temperatures for the *finite length* chains, the second virial coefficient calculation indicates that the chains are in the poor solvent regime, at which chain–chain attractive interactions dominate over the volume exclusion repulsive ones. Even for the longest chain lengths studied (n = 100), the relative difference between the critical temperature and the Boyle temperature is more than 10%.

The Θ point of macromolecules is traditionally viewed as the point at which excluded volume interactions exactly cancel the attractive interactions between monomers of the chain. Consequently, at the Θ temperature chain dimensions behave quasi-ideally, with the radius of gyration proportional to chain length, $\langle R_g^2\rangle \propto n$. Bruns[38] has performed careful simulations on the 5-choice cubic lattice and has determined that the temperature for quasi-ideal chain dimensions coincides, within simulation uncertainty, with the temperature at which the second virial coefficient vanishes at the limit of long chains. Even for the longest chains studied by Bruns (n = 1000), however, there were still detectable deviations from quasi-ideal behavior at the temperature of the vanishing second virial coefficient. No direct comparisons of these temperatures with the critical temperature for phase coexistence are possible for lattice models, because no appropriate phase coexistence results are available. We have followed the scheme of Bruns[38] and have plotted $\langle R_g^2\rangle/\langle R_g^2\rangle_0$ vs $1/T^*$ with $\langle R_g^2\rangle_0 = n(n+2)\sigma^2/6(n+1)$. Straight line segments were used to join successive temperatures for the purpose of locating the intersection temperature. If $\langle R_g^2\rangle$ is proportional to n at some value of T^*, the curves belonging to all chain lengths n will intersect at a single point. As shown in Figure 6, for the chain lengths we have studied, the curves do not intersect at a single point, even for the longest chains. The temperature where two chain lengths intersect increases with chain length. These observations are in agreement with the results of Bruns for lattice chains. The extrapolation of the intersection temperature to chains of infinite chain length is consistent with our calculation of the temperature at which the second virial coefficient vanishes (T^* = 4.43 ± 0.10) and the extrapolation of the critical point to infinite chain lengths (T^* = 4.59). The limiting value of the ratio $\langle R_g^2\rangle/\langle R_g^2\rangle_0$ ($=C_\infty$, the characteristic ratio) at this temperature is approximately 2.5, which is a reflection of local chain stiffness.

IV. Summary and Conclusions

In this paper we have calculated the vapor–liquid equilibrium phase diagrams of a bead–spring chain model ranging in degree of polymerization from oligomers to short polymers by using Monte Carlo simulations. The chain increment method[25] has been applied to overcome the sampling difficulties for estimating chemical potentials in polymeric systems. We found that the calculated phase equilibrium behavior with and without explicitly considering the chain length dependence of the chemical potential shows no difference in liquid side densities, but significant deviations for the vapor phase densities. Our results are in qualitative agreement with experimental data for binary polymer/solvent systems.[32,33] The critical points are estimated by a scaling analysis of the liquid and vapor densities using the rectilinear diameter rule and the scaling relationship for the width of the coexistence curve with the universal value of $\beta = 0.332$. We have found that the dependence of the critical temperature on chain length agrees with the Flory–Huggins[1] prediction, as well as the experimental results.[32]

We have also computed the second virial coefficients for chain–chain interactions as well as the radii of gyration of chains as a function of temperature. We found that the temperatures at which the second virial coefficients vanish are essentially constant for different chain length polymers in our model and the estimated common value agrees, within simulation uncertainty, with the critical temperature for infinite chain length. At the critical points of the finite length polymer chains, the second virial coefficient calculation indicates that attractive chain–chain interactions dominate and the virial coefficient assumes negative values. This is consistent with past expectations and experimental data. We have determined the temperature at which an isolated polymer chain behaves as if it were a random chain (i.e. $\langle R_g^2\rangle \propto n$) and have also found this temperature to coincide within computational uncertainty with the virial coefficient and phase equilibrium determined Θ temperature.

The scheme used in our work can be readily applied to polymers of any length. However, large amounts of computer time will be needed to obtain the phase diagrams of polymers with lengths greater than 100. Reptation and crankshaft moves are not efficient enough for much longer

chain lengths to allow equilibration in a reasonable amount of time. In this respect, the recently developed configurational-bias Monte Carlo methods[8-10] are likely to facilitate internal equilibration of longer polymers. Another possible extension of the present study is to more realistic chain models that take into account variations of the bond lengths, the bond angles, and the torsional angles as well as a Lennard-Jones potential between nonbonded neighbors. The scheme can also be extended to related areas such as the phase equilibria of polymer/solvent systems and polymer/polymer systems. The simulation results would be directly comparable to extensive experimental data on polymer/solvent and theoretical predictions on polymer/polymer immiscibility.

Acknowledgment. At Cornell University, this research is supported by a grant from the Department of Energy (Office of Basic Energy Sciences). Supplemental support has been provided by a National Science Foundation PYI award. A.Z.P. is a Camille and Henry Dreyfus Teacher-Scholar. At Penn State this research is supported in part by a grant from the Petroleum Research Fund. At Purdue this work is partially supported by a grant from Shell Research B.V. (Amsterdam). I.S. is a Camille and Henry Dreyfus New Faculty Awardee. We thank the Pittsburgh Supercomputing Center for Cray C-90 time allocation. A.Z.P. and S.K.K. would also like to acknowledge the hospitality of Prof. Daan Frenkel at FOM where the final manuscript of this paper was completed. We also thank Dr. Grest at Exxon for many valuable discussions.

References and Notes

(1) Flory, P. J. *Principles of Polymer Chemistry*; Cornell University Press: Ithaca, NY, 1953.
(2) Flory, P. J. *J. Chem. Phys.* **1941**, *9*, 660.
(3) Huggins, M. L. *J. Phys. Chem.* **1942**, *46*, 151.
(4) Madden, W. G.; Pesci, A.; Freed, K. F. *Macromolecules* **1990**, *23*, 1181.
(5) Sariban, A.; Binder, K. *J. Chem. Phys.* **1987**, *86*, 5859.
(6) Widom, B. *J. Chem. Phys.* **1963**, *39*, 2808.
(7) Dickman, R.; Hall, C. K. *J. Chem. Phys.* **1988**, *89*, 3168.
(8) Frenkel, D.; Mooij, G. C. A. M.; Smit, B. *J. Phys. Condens. Matter* **1992**, *3*, 3053.
(9) Frenkel, D.; Smit, B. *Mol. Phys.* **1991**, *75*, 983.
(10) de Pablo, J. J.; Laso, M.; Suter, U. W. *J. Chem. Phys.* **1992**, *96*, 6157.
(11) Rosenbluth, M. N.; Rosenbluth, A. W. *J. Chem. Phys.* **1955**, *23*, 356.
(12) Kumar, S. K.; Szleifer, I. Unpublished data.
(13) Panagiotopoulos, A. Z. *Mol. Phys.* **1987**, *61*, 813.
(14) de Pablo, J. J.; Laso, M.; Suter, U. W. *J. Chem. Phys.* **1992**, *97*, 2817.
(15) Siepmann, J. I.; Karaborni, S.; Smit, B. *Nature* **1993**, *365*, 330.
(16) Mazur, J.; McCrakin, F. L. *J. Chem. Phys.* **1968**, *49*, 648.
(17) Baumgartner, A. *J. Chem. Phys.* **1980**, *72*, 873.
(18) Kremer, K.; Baumgartner, A.; Binder, K. *J. Phys. A.* **1981**, *15*, 2879.
(19) Kumar, S. K. *J. Chem. Phys.* **1992**, *96*, 1492.
(20) Szleifer, I.; O'Toole, E. M.; Panagiotopoulos, A. Z. *J. Chem. Phys.* **1992**, *97*, 6802.
(21) Freed, K. F. *Renormalization Group Theory of Macromolecules*; Wiley: New York, 1987.
(22) Yamakawa, H. *Modern Theory of Polymer Solutions*; Harper Row: New York, 1971.
(23) Tsonopoulos, C. *AIChE J.* **1987**, *33*, 2080.
(24) Madden, W. G. *J. Chem. Phys.* **1990**, *92*, 2055.
(25) Kumar, S. K.; Szleifer, I.; Panagiotopoulos, A. Z. *Phys. Rev. Lett.* **1991**, *66*, 2935; **1992**, *68*, 3658.
(26) Allen, M. P.; Tildesley, D. J. *Computer Simulation of Liquids*; Oxford University Press: New York, 1987.
(27) Kumar, S. K. *Makromol. Chem. Macromol. Symp.* **1993**, *65*.
Kumar, S. K. *Fluid Phase Equilib.* **1993**, *29*, 373.
(28) Szleifer, I.; Panagiotopoulos, A. Z. *J. Chem. Phys.* **1992**, *97*, 6666.
(29) Panagiotopoulos, A. Z. *Fluid Phase Equilib.* **1992**, *76*, 97.
(30) Panagiotopoulos, A. Z.; Szleifer, I. *Polym. Prepr. (Am. Chem. Soc., Div. Polym. Chem.)* **1992**, *33* (1), 547-548.
(31) Möller, D.; Fischer, J. *Mol. Phys.* **1990**, *69*, 463.
(32) Dobashi, T.; Nakata, M.; Kaneko, M. *J. Chem. Phys.* **1980**, *72*, 6685.
(33) Shinozaki, K.; van Tan, T.; Saito, Y.; Nose, T. *Polymer* **1982**, *23*, 728.
(34) Panagiotopoulos, A. Z. *Mol. Simul.* **1992**, *9*, 1.
(35) Schultz, A. R.; Flory, P. J. *J. Am. Chem. Soc.* **1952**, *74*, 4760.
(36) de Gennes, P. G. *Scaling Concepts in Polymer Physics*; Cornell University Press; Ithaca, NY, 1991.
(37) Janssens, M.; Bellemans, A. *Macromolecules* **1976**, *9*, 303.
(38) Bruns, W. *Macromolecules* **1984**, *17*, 2826.